Published as: WW Focke, I van der Westhuizen, X Oosthuysen. Biodiesel oxidative stability from Rancimat data. Thermochimica Acta 633 (2016) 116–121. http://dx.doi.org/10.1016/j.tca.2016.03.023

Biodiesel oxidative stability from Rancimat data

Walter W Focke · Isbe van der Westhuizen · Xander Oosthuysen

Highlights
• Sunflower biodiesel was stabilized with a hindered phenol antioxidant.
• Oxidative stability is defined by the length of the Rancimat induction period (IP).
• A novel Rancimat response function allows automated IP determination.
• IP follows an Arrhenius temperature dependence.
• IP increased linearly with antioxidant concentration.

Abstract

It is conventional to quantify the oxidative stability of oils and biodiesel through an induction time determined by a Rancimat instrument. European Standard EN 14112 for the Rancimat method describes two procedures for determining this induction period. The automated method relies on finding the position of the peak in the second derivative of the conductivity vs. time curve. The manual method is based on the intersection of two tangents lines. It is shown that this method can also be automated by a curve fitting approach based on a novel Rancimat response function. This analysis demonstrates that the induction period values determined by the two methods differ with the second derivative method returning slightly higher estimates for the induction period.

Biodiesel was prepared using base-catalysed methanolysis of sunflower oil. It was stabilized using the hindered phenol antioxidant tetrakis[methylene(3,5-di-t-butyl-4-hydroxyhydrocinnamate)]methane. It was found that stability increases linearly with stabiliser concentration and that the effect of the measurement temperature follows Arrhenius kinetics. The effectiveness of the antioxidant stabiliser diminished with increasing temperature.

Keywords: oxidative stability; induction period; Rancimat method; antioxidants; biodiesel

---

Walter W Focke (✉) · Isbe van der Westhuizen · Xander Oosthuysen

Institute of Applied Materials, Department of Chemical Engineering, University of Pretoria, Private Bag X20, Hatfield 0028, Pretoria, South Africa

E-mail: walter.focke@up.ac.za

Introduction

Biodiesel is a renewable fuel produced by reacting vegetable oil or animal fat with methanol in the presence of an alkali catalyst to produce fatty acid methyl esters (FAME). It is more susceptible to oxidative degradation than petroleum diesel as it is contains unsaturated long-chain fatty acids [1, 2]. The oxidative stability can be improved by adding suitable antioxidants [2-4].

Currently the reference method for the measurement of the oxidative stability of biodiesel is EN14112 [5]. It prescribes the Rancimat method [6, 7] for gauging the induction time of the biodiesel. In this procedure autoxidation is accelerated by passing a constant flow of air through the biodiesel sample while controlling the temperature at an elevated level, i.e. 110 °C. The oxidation process is driven by radical reactions that involve the unsaturated fatty acid structures. During an initial induction phase virtually no secondary products are formed. This is abruptly followed by an oxidation phase characterized by a rapid increase in peroxide value and the formation of volatile products. The Rancimat method relies on the fact that the greater part of the volatile matter consists of formic acid. This is trapped by passing the exiting air through distilled water where its accumulation is recorded conductometrically. The length of the induction period (*IP*) is taken as a measure of oxidative stability. EN14112 [5] describes two methods for the evaluation of the *IP* from a conductivity vs. time curve. An example is shown as an insert in Figure 1(a). Furthermore, there is a tacit assumption that the two methods yield comparable if not identical results. The "manual method" relies on the determination of the point of intersection of two optimal tangents to the conductivity vs. time curve. The first tangent is drawn along the first, moderately increasing part of the curve. The second is drawn along the upper part of the rapidly increasing portion of the curve. The problems associated with this manual approach is that it is operator dependent. It relies on subjective judgment of the "optimal" tangents. The "automatic method" identifies the *IP* with the location of the position of the maximum in the second derivative of the conductivity vs. time curve. Determining the second derivative from noisy data is not a simple problem, in fact it is considered to be an ill-posed problem [8]. Occasionally problems are experienced with this method too [9]. For example, the second derivative generated by the instrument from the conductivity-time curve may show multiple maxima and it then becomes necessary to revert to the "manual method" [9].

The main objective of this communication was to explore ways to automate the "manual method" for evaluating the *IP* from the Rancimat curves and to critically compare the results returned by the two methods. If this can be done, the corresponding *IP* value can be generated directly by the instrument software without operator intervention. Another objective of this study was to study the stabilization of sunflower oil-based

biodiesel with a hindered phenol antioxidant at different dosage levels. The oxidation stability of the sunflower biodiesel was also tested at different temperatures using the Rancimat method.

Materials and Methods

Materials

Pure triple distilled sunflower oil was manufactured by Sunfoil. The antioxidant considered was the hindered phenol tetrakis[methylene(3,5-di-t-butyl-4-hydroxyhydrocinnamate)]methane (Anox 20 ex Addivant). The antioxidant was added to the biodiesel at different loadings up to a maximum of 0.25 wt.%.

Biodiesel preparation

The biodiesel was prepared at ambient conditions (28 °C ± 2 °C) from sunflower oil using the following procedure: A catalyst, potassium hydroxide, was dissolved in 100 mL of dry methanol. The solution was then poured over 500 mL of the sunflower oil in a large Mason jar. The jar was securely closed and the solution vigorously agitated for 15 minutes. The solution was then transferred to a gravity separation funnel and allowed to settle. In the first hour the separation appeared about 75% complete. After 8 h the glycerine reaction product had settled at the bottom with a biodiesel or FAME layer on top. The lower glycerol phase was removed. The FAME was then washed to remove residual catalyst, free fatty acids and methanol. The product was washed five times with 140 mL distilled water portions. The biodiesel was then placed in an open container in a convection oven at 70 °C to remove the remaining methanol and water. After drying the biodiesel sample was stored in airtight container in a fridge.

Characterization

The fatty acid methyl ester (FAME) analysis was performed by Analytical Services, Food and Beverage Laboratory, CSIR on an Agilent 6890 GC-FID. An Agilent J&W GC column CP-SIL 88 (100 m × 0.25 mm ϕ with a film thickness of 0.20 μm) was used for the separation of the FAME's. The column temperature was initially set at 60 °C for 1 minute, and then stepwise increased first to 150 °C at a rate of 20 °C min^{-1}, then to 215 °C at a rate of 5 °C min^{-1} and finally to 240 °C at a rate of 1.5 °C min^{-1} where it was held constant for 40 min. Hydrogen was used as the carrier gas with hydrogen and air as fuel gases. Injector and detector

temperatures were 230 °C and 260 °C respectively. Injection volumes for samples and standards were 1 µL and a split ratio of 150:1 was employed.

The biodiesel sample was dissolved in heptane and quantification was performed by internal standard calibration using methyl heptadecanoate. The FAME content was computed according to EN 14103 [10] and [11] where the sum of all the peaks from the methyl myristate (C_{14}) peak up to that of the methyl ester in $C_{24:1}$ was accounted for. Identification of the FAMEs in the biodiesel samples was accomplished by comparing their retention times to a Supelco FAME reference mixture containing 37 components.

FTIR spectra of the neat biodiesel was obtained using KBr plates on a Perkin Elmer Spectrum RX I FTIR spectrometer. The reported spectrum represents the average of 12 scans recorded at a resolution of 2 cm^{-1}.

Additional physical properties of the biodiesel samples were determined, using standard procedures, by Bio Services CC, Randburg, South Africa. These included total glycerine, free glycerine, methanol content, water content, acid value, iodine value and flash point.

Antioxidant formulations and determination of the oxidative induction times

The effect of antioxidant concentration on the induction time was determined by spiking the biodiesel with different amounts of Anox 20 as indicated in Table 3. The variation of the induction time with temperature was studied at 80, 90, 100, 110 and 120 °C.

The oxidation stability of the neat biodiesel as well as the stabilised biodiesel samples was determined using a Metrohm 895 Professional PVC Thermomat. It was set up with the required accessories to analyse biodiesel according to the EN14112 [5] Rancimat method. A typical procedure was as follows: The cellblock temperature was ramped to 110 °C and held constant. A 3.00 g biodiesel sample was transferred into the reaction vessel and placed in the cellblock. The air flow rate was set at 10 L h^{-1}. It was passed through the sample and then through a measuring vessel containing 50 mL of deionised water. The increase in conductivity was measured as a function of time. The Rancimat induction time (IP_R) was determined automatically using the instrument software using the second derivative method. Repeat measurements of the induction time were carried out for each sample.

Data reduction

The Rancimat produces data corresponding to the initial part of the oxidation reaction. The induction time values were extracted from the experimental conductivity vs. time data generated by the Rancimat instrument as follows. It was assumed that the conductivity vs. time curves ($\sigma = \sigma(t)$) could be represented by the following equation:

$$\sigma(t) = \sigma_{min} + mt + \beta F(t) \qquad (1)$$

where $\sigma(t)$ is the experimental conductivity vs. time curve; σ_{min} is the conductivity offset at time $t = 0$; m is the slope of the initial portion of the conductivity curve; β is a proportionality constant and $F(t)$ is the response function. Note that the parameter m in equation (1) compensates for any linear signal drift over the full measurement time. The response function $F(t)$ should be able to adequately represent the experimental data over the full measurement range. Inspection showed that the following empirical expression was adequate for the present data set:

$$F(t) = log[1 + (t/\tau)^{\theta}] \qquad (2)$$

where t is the time in h, "*log*" represents the natural logarithm while θ and τ are adjustable model parameters.

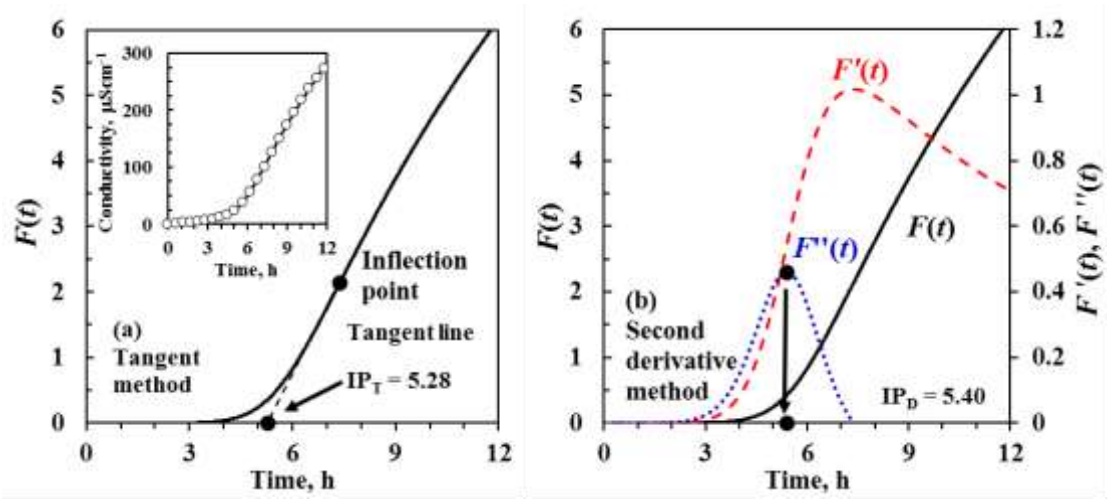

Figure 1. Schematic illustration of the data reduction methods used. The experimental conductivity vs. time curves (insert in (a)) were fitted to the response function $F(t)$ defined by equation (1). The parameter values were determined from the experimental data using least square fits. The *IP* values were directly determined from the sigmoidal response curves parameters based on two different methods: (a) the first approach is based on the assumption that the IP corresponds to the intersection, with the time axis, of the tangent line drawn to the inflection point of $F(t)$; (b) The second methodology associates the *IP* with the position of the maximum in the second derivative of $F(t)$, i.e. $F''(t)$.

The adjustable parameters that characterise the analytic expression for $F(t)$ and the values of both m and σ_{min} were determined by least square fits to the experimental data. Figure 1 graphically illustrates how the induction periods (IP_T and IP_D) were determined from the fitted response curves. The "manual method" described in EN14112 [5] corresponds to the procedure shown in Figure 1(a). The IP_T corresponding to the "manual" method is defined by the intersection of the tangent line drawn to the inflection point [12] of the normalized dose-response curve with the time axis. The "automatic instrument" procedure mentioned in EN14112 [5] is illustrated in Figure 1(b). IP_D is established by finding the position of the maximum in the second derivative of the fitted $F(t)$ curve. The experimental Rancimat IP_R values were obtained by the instrument software in a similar fashion. The only difference is that in this case the second derivative was directly obtained from the raw numerical data. However, it is quite clear that some (unknown) data smoothing procedures must have been in operation.

Figure 1 explains the underlying principles defining the induction periods graphically. However, the actual calculations of the *IP* values were done using the parameters of the analytical dose-response expressions. The relevant response function derivatives, and the corresponding expressions for the parameters required to evaluate the induction periods, are listed in Table 1.

Table 1. Analytic expressions for the response function, its derivatives and some of its properties

Response function expressions	
$F(t) = log[1 + (t/\tau)^{\theta}]$	
$F'(t) = n(t/\tau)^{\theta}/\{t[1 + (t/\tau)^{\theta}]\}$	
$F''(t) = n(t/\tau)^{\theta}[1 - n + (t/\tau)^{\theta}]/\{t[1 + (t/\tau)^{\theta}]\}^2$	
$F'''(t) = n(t/\tau)^{\theta}[2 - 3n + n^2 + (4 - 3n - n^2)(t/\tau)^{\theta} + 2(t/\tau)^{2\theta}]/\{t[1 + (t/\tau)^{\theta}]\}^3$	
Parameter	**Expression**
Response function inflection point	$t_i = \tau(\theta - 1)^{1/\theta}$
Slope at inflection point	$F'(t_i) = (\theta - 1)^{(\theta-1)/\theta}/\tau$
Tangent line abscissa intercept (defines IP_T)	$t_0 = \tau(\theta - 1)^{1/\theta}[1 - log(\theta)/(\theta - 1)]$
Position of the maximum in the second derivative curve (defines IP_D)	$t_D = \tau\left[(1/4)\left(\theta^2 + \left(3 - \sqrt{\theta^2 + 6\theta - 7}\right)\theta - 4\right)\right]^{1/\theta}$

For the present study it was assumed that the Rancimat instrument *de facto* generated "true" induction time values (IP_R). These values are, in effect, based on a single data point corresponding to the condition where the second derivative attained a maximum value. In contrast, the IP_D and IP_T are global values as they are based on all the available experimental data points. Therefore, they were directly determined from the adjustable

parameters, θ and τ, of the analytical expression for $F(t)$ used to model the data trends. Those, in turn were determined by fitting the dose-response curve considering all the available experimental data points.

Results

Biodiesel characterization

The total fatty acid methyl ester (FAME) content and the composition of the sunflower biodiesel are listed in Table 2 together with other physical properties. Biodiesel Batch 1 was used to study the effect of temperature while biodiesel Batch 2 was used to study the effect of antioxidant concentration on the induction time (*IP*). The FTIR spectrum (Figure 2) of the present biodiesel featured a strong band at 1740 cm^{-1} corresponding to the ester carbonyl functionality. The three strong bands at 1100 cm^{-1}, 1740 cm^{-1} and 2900 cm^{-1} are characteristic of FAME biodiesel. The absence of absorption bands in the 3500 – 3200 cm^{-1} or 3640 – 3610 cm^{-1} ranges [13] confirmed that the sample was free of residual alcohol and glycerol.

Table 2. Biodiesel FAME content and ester composition

Biodiesel property	**Batch 1**	**Batch 2**
FAME (ester content) (wt.%)	92.5	98.3
FAME composition: (%)		
• Methyl palmitate, C16:0 (saturated)	6.29	6.73
• Methyl stearate, C18:0 (saturated)	6.45	6.63
• Methyl oleate, C18:1 (mono unsaturated)	21.8	22.4
• Methyl linoleate, C18:2 (polyunsaturated)	63.0	62.0
• Methyl linolenate, C18:3 (polyunsaturated)	0.37	0.22
• Other methyl esters	2.09	2.02
Density at 15°C (kg m^{-3})	n.d.	888
Viscosity at 40°C (mm^2s^{-1})	n.d.	4.6
Flash point (°C)	170	170
Water content (%)	0.05	0.04
Acid value (mg KOH g^{-1})	0.1	0.1
Methanol content (%)	0	0
Iodine value (g I_2 (100 g biodiesel)$^{-1}$)	119	118
Free glycerol (%)	0.02	0.01
Appearance	clear	clear

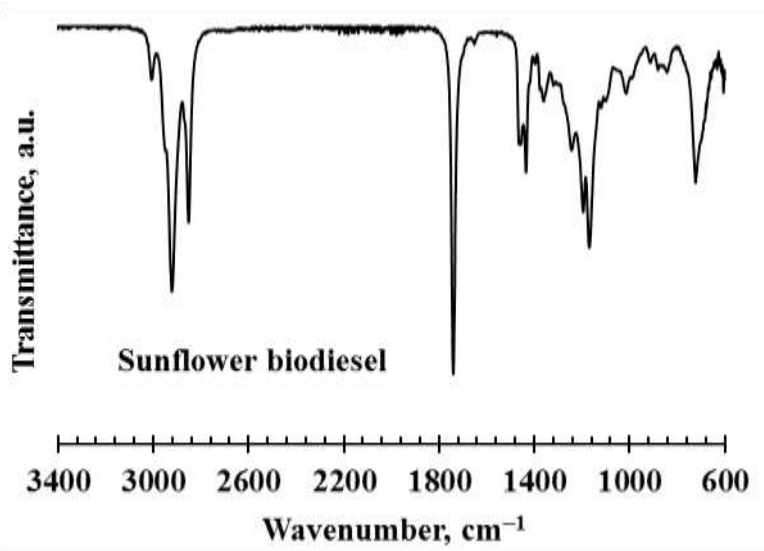

Figure 2. FTIR spectrum of the sunflower biodiesel Batch 2

Oxidative induction periods from global Rancimat data analysis

Figure 3(a) shows representative Rancimat conductivity vs. time curves. The symbols display selected experimental data points and the solid lines represent fits obtained with the response model defined in equation (1). The model parameters include a characteristic time constant (τ) while the dimensionless parameter θ affects the shape of the response curve. The response functions extracted from the corresponding data sets are plotted in Figure 3(b). In all cases eyeballing indicated that good data fits were obtained. Induction time estimates, based on the two different methods, were calculated using the fit parameters of these models using the expressions listed in Table 1.

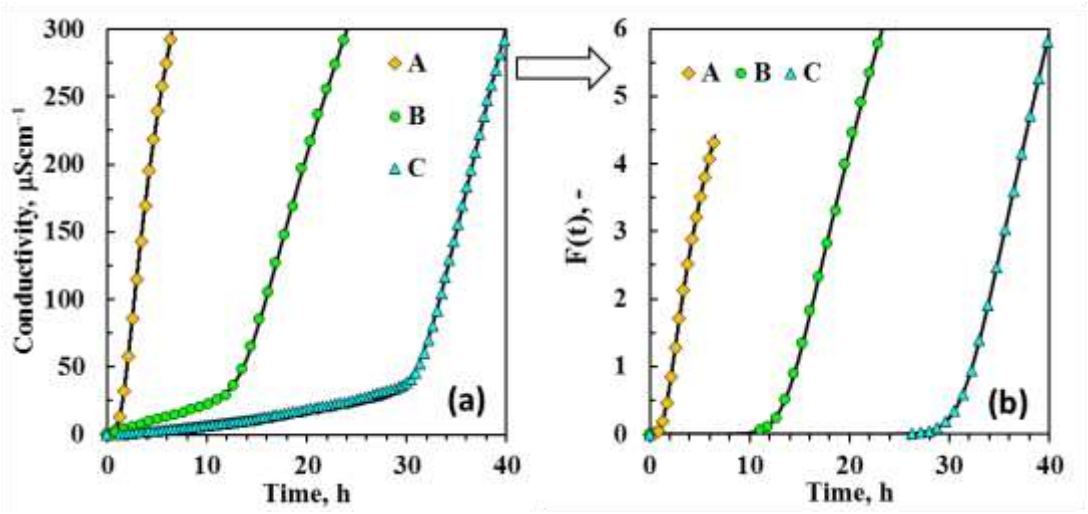

Figure 3. (a) Representative Rancimat conductivity vs. time curves with **(b)** the corresponding response functions extracted from the raw data. A: Neat biodiesel at 120 °C. B and C: Biodiesel spiked with 0.15 wt.% Anox 20 at 100 °C and 90 °C respectively.

Table 3. Effect of antioxidant (Anox 20) concentration on the induction period of sunflower biodiesel.

C, wt.%	IP_R	IP_T	IP_D	IP_R/IP_T	IP_R/IP_D	IP_D/IP_T
0	1.56	1.56	1.56	1.00	1.00	1.00
0	1.53	1.53	1.53	1.00	1.00	1.00
0	1.53	1.53	1.53	1.00	1.00	1.00
0.083	3.67	3.56	3.64	1.03	1.01	1.02
0.083	3.76	3.92	4.01	0.96	0.94	1.02
0.083	3.77	3.92	4.01	0.96	0.94	1.02
0.125	4.32	4.47	4.58	0.97	0.94	1.03
0.125	4.32	4.60	4.72	0.94	0.92	1.03
0.125	4.73	4.68	4.80	1.01	0.99	1.03
0.150	4.20	4.17	4.28	1.01	0.98	1.03
0.150	4.08	4.11	4.18	0.99	0.98	1.02
0.150	4.83	4.72	4.83	1.02	1.00	1.02
0.167	5.11	5.23	5.37	0.98	0.95	1.03
0.167	5.19	5.29	5.42	0.98	0.96	1.03
0.167	5.42	5.45	5.58	1.00	0.97	1.02
0.250	5.56	5.50	5.64	1.01	0.99	1.03
0.250	6.92	6.48	6.65	1.07	1.04	1.03
0.250	6.49	6.35	6.50	1.02	1.00	1.02

The instrument IP_R values, determined by the Rancimat instrument software, are listed in Table 3 and plotted in Figure 4 against the *IP* values derived from the model parameters. It is evident from Figure 4 that the IP_T and IP_D values extracted from global data fits are in good agreement with the IP_R values generated by the Rancimat software. The IP_T values generated by the intersecting tangent method apparently yielded values that were almost identical to those determined by the Rancimat software from the raw data. Taking all the data points together, a relationship, corresponding to a direct proportionality, was found: $IP_R = k\, IP_T$ with $k = 0.995 \pm 0.038$. In contrast, the IP_D values, based on the second derivative method, are slightly higher. Here it was found that in this case $k = 0.976 \pm 0.039$. This means that the calculated IP_D values were, on average, about 2.5 % higher than the IP_R values. The excellent agreement between the IP_T values obtained via curve fitting with those obtained from the instrument could provide a way to automate the manual method described in the EN 14112 Standard for the Rancimat method. However, while this was certainly true for the present data set, further investigation and testing will be necessary before this can be contemplated as a general approach.

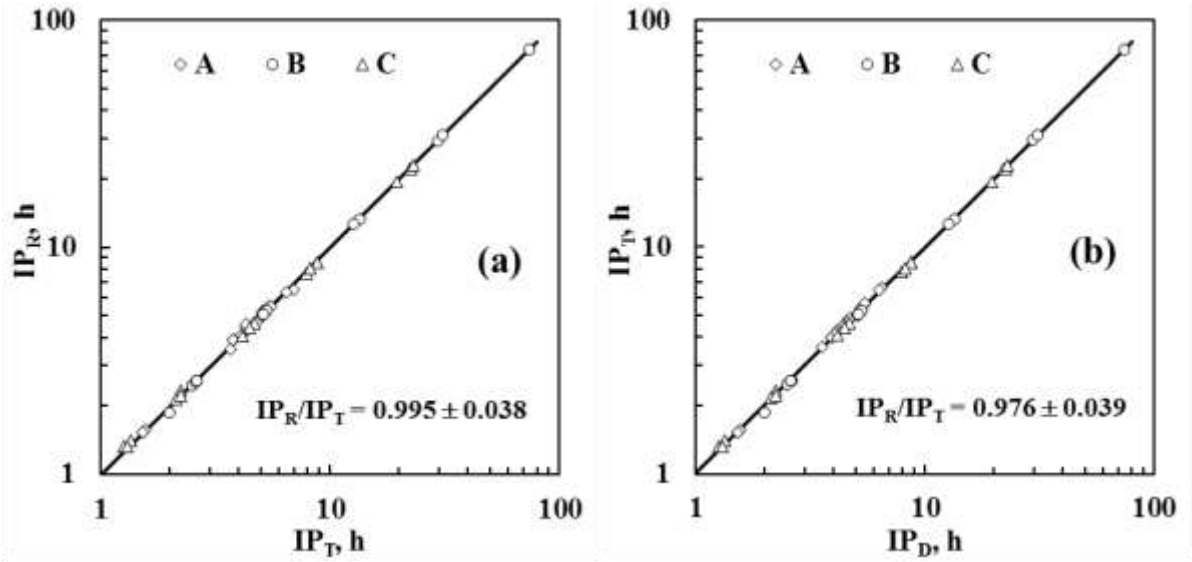

Figure 4. Comparing the model-based induction times to those reported by the software installed on the Rancimat instrument. (a) IP_R vs. IP_T, and (b) IP_T vs. IP_D. A: Different Anox 20 concentrations; B: Biodiesel with 0.15 wt.% Anox at different temperatures, and C: Neat biodiesel at different temperatures.

Effect of antioxidant dosage level

Table 3 lists the effect of antioxidant concentration on the experimental induction times. Figure 5 shows a plot of the induction time IP_T vs. the concentration of the antioxidant Anox 20. The *IP* values increase linearly with antioxidant concentration according to:

$$IP = IP_o + K\,C \qquad (3)$$

where *IP* and IP_o are the induction times in h of the stabilised and the neat biodiesel respectively, *C* is the concentration of the antioxidant in wt.% and *K* is a proportionality constant. The value of this constant for the tangent-based induction time was $K = 21.2 \pm 3.5$ h $(\text{wt.\%})^{-1}$. This means that, for biodiesel Batch 2 with IP_o = 1.56, equation (3) predicts that an extrapolated antioxidant dosage exceeding 0.30 wt.% is required in order to conform with the 8 h stability requirement of EN14112 [5]. However, a little more than 0.07 wt.% will suffice to pass the 3 h ASTM D6751 [14] specification.

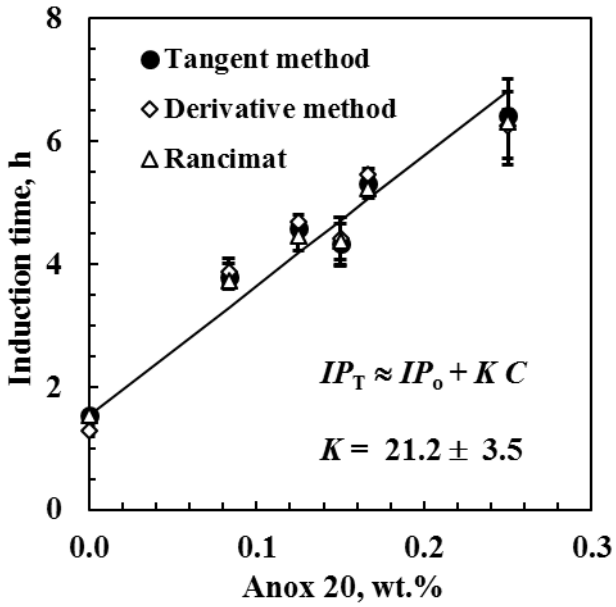

Figure 5. The effect of antioxidant (Anox 20) concentration on the induction time.

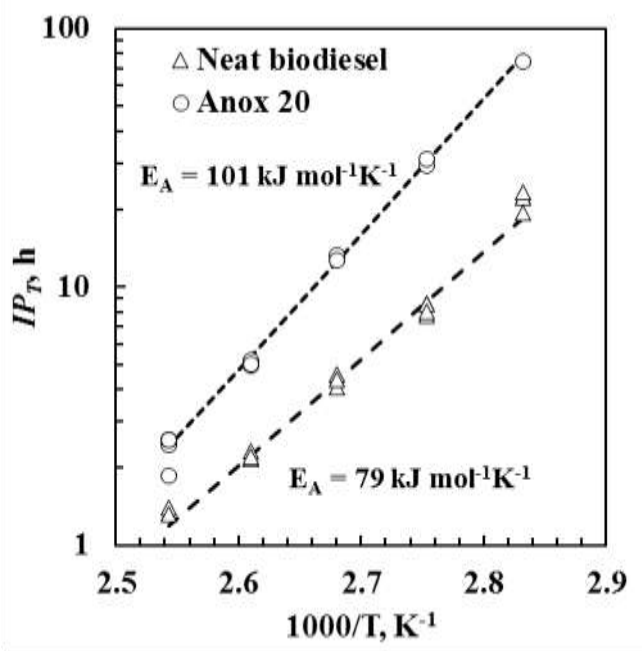

Figure 6. The effect of measurement temperature on the induction time for neat biodiesel Batch 1 and a sample spiked with 0.15 wt.% antioxidant (Anox 20).

Effect of measurement temperature

Table 4 lists and Figure 6 shows the effect of measurement temperature on the induction time for neat biodiesel Batch 1 and a sample spiked with 0.15 wt.% antioxidant (Anox 20). The IP_T values for both fluids followed an Arrhenius temperature dependence:

Table 4. Effect of measurement temperature on the induction period of neat sunflower biodiesel and a sample spiked with 0.15 wt.% Anox 20 antioxidant.

T, °C	IP_R	IP_T	IP_D	IP_R/IP_T	IP_R/IP_D	IP_D/IP_T
Neat biodiesel						
80	21.9	22.1	22.2	0.99	0.99	1.00
80	20.9	19.3	19.6	1.08	1.06	1.02
80		22.2	22.5			1.01
80		23.1	23.0			1.00
90	8.0	8.5	8.8	0.94	0.92	1.03
90	7.4	8.6	8.8	0.87	0.85	1.02
90		7.7	7.9			1.03
90		8.0	8.2			1.02
100	4.7	4.6	4.7	1.02	1.00	1.02
100	4.0	4.1	4.1	0.98	0.96	1.02
100	4.1	4.4	4.5	0.92	0.90	1.02
110	2.1	2.3	2.2	0.92	0.95	0.97
110	2.2	2.1	2.1	1.01	1.02	0.99
110		2.2	2.2			1.01
120	1.3	1.3	1.3	1.01	1.05	0.96
120	1.3	1.4	1.3	0.94	0.97	0.96
120	1.3	1.3	1.3	0.96	0.97	0.99
Anox 20 @ 0.15 wt.%						
80	73.6	74.2	74.8	0.99	0.99	1.01
90	31.1	29.4	29.6	1.06	1.05	1.01
90	29.4	31.1	31.3	0.94	0.94	1.01
100	12.5	13.2	13.5	0.94	0.93	1.02
100	12.3	12.6	12.8	0.98	0.97	1.01
110	5.5	5.2	5.4	1.06	1.03	1.03
110	5.0	5.0	5.1	1.01	0.99	1.03
110	5.2	5.0	5.1	1.04	1.01	1.03
120	2.4	2.5	2.5	0.99	0.97	1.03
120	2.7	2.6	2.6	1.04	1.01	1.03
120	2.4	2.5	2.6	0.94	0.91	1.03
120	2.3	2.6	2.6	0.91	0.89	1.03

$$IP_T(T) = A_T exp[E_T/RT] \quad (3)$$

where $IP_T(T)$ is the induction time in h at temperature T in K; A_T is the pre-exponential factor with units of h; E_T is the activation energy in J $mol^{-1}K^{-1}$, and R is the gas constant (approximately 8.3145 J $mol^{-1}K^{-1}$). The activation energies for the neat biodiesel and the stabilised sample were calculated as 79 and 101 kJ $mol^{-1}K^{-1}$, respectively. This means that the stabilising effect of the antioxidant diminishes with increasing temperature.

This is also evident from the plots in Figure 6. A previous study [15], on propyl gallate-stabilised safflower biodiesel, also found that the Rancimat *IP* values obey Arrhenius-like temperature dependence. These authors observed an activation energy of 97 kJ $mol^{-1}K^{-1}$, which is similar to the present value for the stabilised biodiesel.

Conclusions

The manual method for determining Rancimat induction times (*IP*) described in standard EN14112 [5] can be automated using software that fits a novel dose response model to the Rancimat conductivity vs. time data. This allows global evaluation of the induction time, from the model fit parameters, using both the tangent and second derivative methods. However, the analytical expressions and the actual data clearly indicate that the two methods yield slightly different IP values. For the present data set the second derivative method yielded *IP* values that were about 2.5% longer than those calculated using the tangent method.

The hindered phenol-type antioxidant, tetrakis[methylene(3,5-di-t-butyl-4-hydroxyhydrocinnamate)]methane was investigated as a stabiliser for sunflower biodiesel. The oxidative stability of neat and stabilised samples, quantified using the Rancimat induction period (IP_R), increased linearly with antioxidant concentration and showed Arrhenius-like dependence on the measurement temperature.

Acknowledgements

Financial support for this research, from the Energy Institutional Research Theme of the University of Pretoria, is gratefully acknowledged.

Conflicts of interest

The authors declare that there are no conflicts of interest to disclose.

References

[1] G. Karavalakis, S. Stournas, D. Karonis, Evaluation of the oxidation stability of diesel/biodiesel blends, Fuel, 89 (2010) 2483-2489.
[2] G. Knothe, Some aspects of biodiesel oxidative stability, Fuel Processing Technology, 88 (2007) 669-677.
[3] S. Jain, M.P. Sharma, Stability of biodiesel and its blends: A review, Renewable and Sustainable Energy Reviews, 14 (2010) 667-678.
[4] S. Schober, M. Mittelbach, The impact of antioxidants on biodiesel oxidation stability, European Journal of Lipid Science and Technology, 106 (2004) 382-389.

[5] European Standard EN 14112, Fat and oil derivatives-Fatty Acid Methyl Esters (FAME)-Determination of oxidation stability (accelerated oxidation test), in, 2003.
[6] H.Z. Hadorn, K., Zur bestimmung der oxydationsstabilität von ölen und fetten, Deutsche Lebensmittel-Rundschau, 70 (1974) 57-65.
[7] M.W. Läubli, P.A. Bruttel, Determination of the oxidative stability of fats and oils: Comparison between the active oxygen method (AOCS Cd 12-57) and the rancimat method, Journal of the American Oil Chemists' Society, 63 (1986) 792-795.
[8] H. Xu, J. Liu, Stable numerical differentiation for the second order derivatives, Advances in Computational Mathematics, 33 (2010) 431-447.
[9] M. Lapuerta, J. Rodríguez-Fernández, A. Ramos, B. Álvarez, Effect of the test temperature and anti-oxidant addition on the oxidation stability of commercial biodiesel fuels, Fuel, 93 (2012) 391-396.
[10] European standard EN 14103, Fat and oil derivatives-Fatty Acid Methyl Esters (FAME)-Determination of ester and linolenic acid methyl ester contents, in, 2011.
[11] T. Ruppel, T. Huybrighs, Fatty Acid Methyl Esters in B100 Biodiesel by Gas Chromatography (Modified EN 14103).
[12] P.K. Fearon, S.W. Bigger, N.C. Billingham, DSC combined with chemiluminescence for studying polymer oxidation, Journal of Thermal Analysis and Calorimetry, 76 (2004) 75-83.
[13] J. Coates, Interpretation of Infrared Spectra, A Practical Approach, in: R. Meyers (Ed.) Encyclopedia of Analytical Chemistry, John Wiley & Sons Ltd, Chichester, 2000, pp. 10815-10837.
[14] A. D6751-15ce1, Standard Specification for Biodiesel Fuel Blend Stock (B100) for Middle Distillate Fuels, in, ASTM International, West Conshohocken, PA, 2015.
[15] J. Xin, H. Imahara, S. Saka, Kinetics on the oxidation of biodiesel stabilized with antioxidant, Fuel, 88 (2009) 282-286.